UKRAINIAN JOURNAL OF MECHANICAL ENGINEERING AND MATERIALS SCIENCE
Vol. 10, No. 4, 2024

Iaroslav Lavrenko[1], Tetiana Sydora[2]

[1] Department of Dynamics and Strength of Machine and Strength of Materials, National Technical University of Ukraine "Ihor Sikorsky Kyiv Polytechnic Institute", 37, Prospect Beresteiskyi (former Peremohy), Kyiv, Ukraine, E-mail: lavrenko.iaroslav@gmail.com.ua, ORCID 0000-0002-4384-4866,
[2] Department of Dynamics and Strength of Machine and Strength of Materials, National Technical University of Ukraine "Igor Sikorsky Kyiv Polytechnic Institute", 37, Prospect Beresteiskyi (former Peremohy), Kyiv, Ukraine, E-mail: tania.sydora@gmail.com, ORCID 0009-0001-9832-9941

STRENGTH INVESTIGATION OF A STRUCTURAL ELEMENT OF A LABORATORY CENTRIFUGE

Received: October 22, 2024 / Accepted: December 6, 2024

https://doi.org/

Abstract. The rotor is a major element of high-speed mechanisms that are widely used in various industries, such as laboratory centrifuges for separating mixtures of different fractions, gas turbines, industrial compressors, engines, and others. The main requirement for such mechanisms is reliability and safety during operation. To ensure the above requirements, it is necessary to determine the stress-strain state of the most loaded structural elements of the system. This paper presents an analysis of the stress-strain state of the rotor system shaft using the example of a Pico21 laboratory centrifuge. ANSYS and KISSsoft software packages were used for 3D modeling of the finite element model. The rotor system consists of a flexible shaft with a rotor, the mass of which was changed during the simulation, and supports, the role of which is played by bearings. This paper presents a comparative analysis of the obtained results of the stress-strain state depending on the mass of the rotors, which further makes it possible to perform appropriate calculations taking into account design features to determine the durability and service life of high-speed mechanisms. The paper presents the results of determining the safety factors depending on the mass of the rotors used in a laboratory centrifuge. The analysis of the safety factors determined with the software packages Ansys, KISSsoft, and analytical methods was carried out.

Keywords: Centrifuge, stress, strain, fatigue, ANSYS, KISSsoft, safety factor.

Introduction

Most structural elements of modern machines and mechanisms operate under variable loads that cause vibration. Vibrations cause cyclic stresses that cause damage and fatigue failure, especially in the case of resonance or other transient states. Unstable states, in turn, impair the functionality of structures.

The design of modern mechanisms and machines is developing in the direction of increasing power and high speeds while reducing weight. At the same time, dynamic loads are increasing, and the vibration impact on mechanisms, tools, and their structural elements is increasing accordingly.

Problem statement

The moving parts of laboratory centrifuges pose a potential risk of failure during operation. To operate such structures, several requirements are imposed on them to ensure safety and reliability during the guaranteed service life. These requirements are ensured by the fact that the rotating elements of the structure must not be damaged during the guaranteed service life, as well as by the presence of a protective shell, which leads to an increase in the weight of the centrifuge.

Centrifuge manufacturers need to experimentally confirm that the centrifuge shell guarantees that all mechanical components and material samples will remain in the centrifuge in the event of the most dangerous failure, but such studies are quite expensive. In this regard, studying the strength of the most loaded structural elements of laboratory centrifuges using software systems is relevant. The safety factor provides additional structural reliability to avoid damage and destruction in the event of possible design, manufacturing, or operational failures. One of these structural elements is a centrifuge shaft with rotors of different masses.

Review of Modern Information Sources on the Subject of the Paper

In the realm of structural and mechanical engineering, the effective management of fatigue failure is a critical aspect in ensuring the reliability and durability of various components subjected to mechanical loads.

In paper [1], the authors introduced a new method for optimizing the layout of mechanical structures under constant and proportional loads, considering both dynamic fatigue and static failure criteria. In [2], the study analyzes the failure of a hydraulic cylinder rod used in fatigue testing large cables for marine applications. The rod, made of 42CrMo4 steel, fractured during a test, and the paper assesses the failure using conventional and DIN 743 analyses, providing insights for engineering applications.

A novel fatigue model validated through experiments for threaded fasteners, considering mean stress impact on high-cycle fatigue is presented in [3, 4]. Comparative analyses with existing models are conducted using commercially available threaded fasteners. In [4, 5], the authors argue that the Goodman and Soderberg equations significantly underestimate cycle-to-failure when dealing with fatigue data with non-zero mean stress.

Comparison fatigue analysis methodologies for rotating steel shafts, focusing on Soderberg and DIN 743 approaches is shown [5]. The study reveals substantial differences between the two methodologies in a common case involving a diameter transition in a steel shaft under bending and torsion moments. In paper [6] investigates the influence of mean shear stress on the torsional fatigue behavior of steel, proposing an extension of Crossland's theory.

Authors [7] explore fatigue behavior in pre-strained corners of stainless steel sheets, presenting bending fatigue tests and proposing fatigue limit predictions using Gerber and Goodman methods. Reevaluates the Haigh diagram, considering creep damage on the high-cycle fatigue behavior of alloy 617M is shown by authors in [8].

In [9, 10], a historical review of constant life diagrams used in fatigue design is presented, distinguishing between engineering curve fits and dynamic theory approaches. In [11, 12] authors analyze the structural integrity of screws in a turbo-diesel engine's crankshaft, focusing on fatigue as the primary failure mode. The study uses Goodmans and Gerbers diagrams for evaluation.

A concept for material selection based on damage tolerance during manufacturing, proposing a static equivalent to the Kitagawa – Takahashi diagram for the bending process introduced in [13, 14]. Changes in plastic deformation properties impact fatigue strength through fatigue-ratcheting interaction, proposing a modification of the Goodman relation aligned with experimental results discussed in [15, 16, 17].

In view of the above, the study of fatigue of materials is an important task in engineering. When conducting research, an important aspect is to consider various types of rotors, such as fixed angle rotors, variable angle rotors, variable volume rotors, and rotors for microtubes and microtiles. Fixed-angle rotors have a constant angle of inclination of the samples to the rotation axis, contributing to efficient material separation. Variable-angle rotors can provide more flexibility in selecting the sample angle, which is useful for different types of materials and experiments. Each type has its own characteristics, such as sample volume and number, rotational speed, design features, etc.

The study of rotors and their characteristics allows us to determine their efficiency and application in specific areas. Large, high-volume rotors can be used to process large volumes of material, while microtile rotors can be useful for molecular biology and genetics research.

When designing and using centrifuges, it is necessary to consider the structures' strength and stability limits. For this purpose, safety factors are calculated to ensure the safety and reliability of centrifuges under various operating conditions. The safety factors ensure that the rotors can withstand maximum loads without damage and provide reliable operation for sample preparation.

Objectives and Problems of Research

To predict the lifetime of structural elements, it is necessary to determine their stress-strain state (SSS) more accurately. Since full-scale tests are quite expensive, numerical modeling using the FEM is an actual task.

The aim of this work is to study the stress-strain state on the example of a real shaft structure of a Pico21 laboratory centrifuge, taking into account the influence of rotors of different masses, in order to identify dangerous areas at the design stage and reduce manufacturing time. It is also important to determine the safety factor, which makes it possible to guarantee the safety and reliability of centrifuges under various operating conditions.

Main material presentation

Laboratory centrifuges are designed to separate mixtures into fractions of different densities. In this paper, we consider the shaft of a Pico 21 laboratory centrifuge manufactured by Thermo Scientific Electron Corporation, to which rotors of different configurations and weights are attached (Fig. 1).

a *b*

Fig. 1. Laboratory centrifuge with rotor: a – Pico 21 centrifuge; b – different rotor configurations

In the paper, the problem of determining the stress-strain state (SSS) of a centrifuge shaft with different rotor weights (0.3–0.7 kg, 1.5–2.7 kg) was studied by numerical methods using the popular software packages ANSYS and KISSsoft.

To model the shaft, we used steel 45, the characteristics of which are shown in Table 1.

Table 1

Material properties

Parameter	Units of measure	Value
Density	kg/m^3	7850
Thermal expansion coefficient	C^{-1}	1.2×10^{-5}
Young modulus	Pa	2×10^{11}
Poisson's ratio		0.3
Shear modulus	Pa	7.6923×10^{10}

A drawing of the shaft, which was calculated in ANSYS and Kisssoft software packages, is shown in Fig. 2.

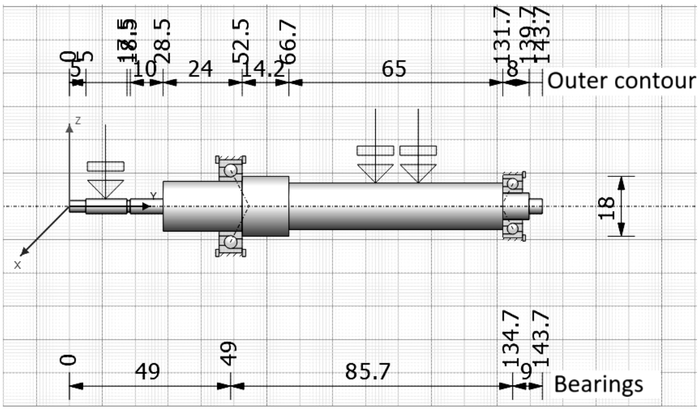

Fig. 2. Centrifuge shaft drawing in the KISSsoft software package

1. Numerical modeling of the stress-strain state of a laboratory centrifuge shaft using the ANSYS and KISSsoft software package

The numerical modeling of the stress-strain state of the centrifuge shaft (Fig. 2) was performed in ANSYS and KISSsoft with the corresponding material characteristics presented in Table 1 and rotor masses.

Since the von Mises criterion gives more accurate calculation results, Fig. 3 shows graphical dependences of stresses and displacements on rotor masses obtained in ANSYS and Kisssoft, accordingly.

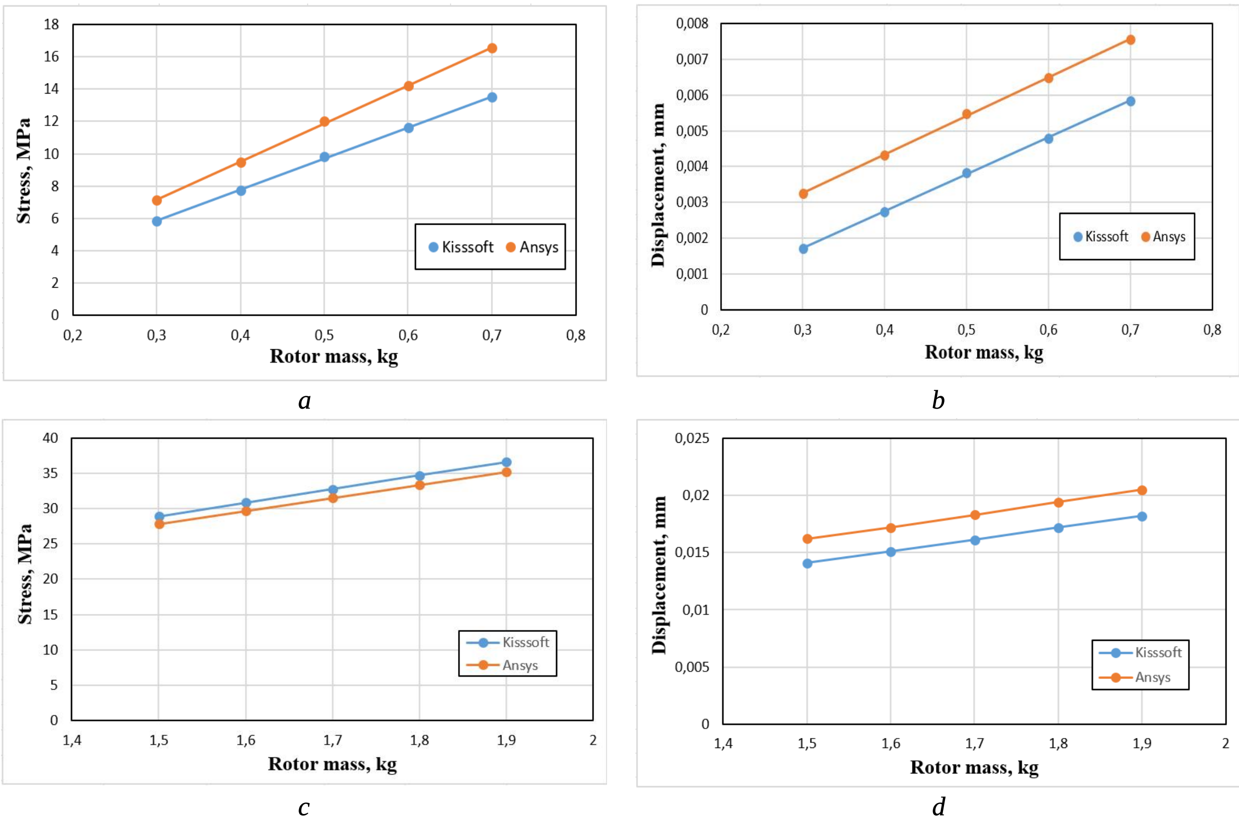

Fig. 3. Equivalent stresses *(a, c, e, g)* and total displacements *(b, d, f, h)* calculated for rotors of different masses using KISSsoft and ANSYS

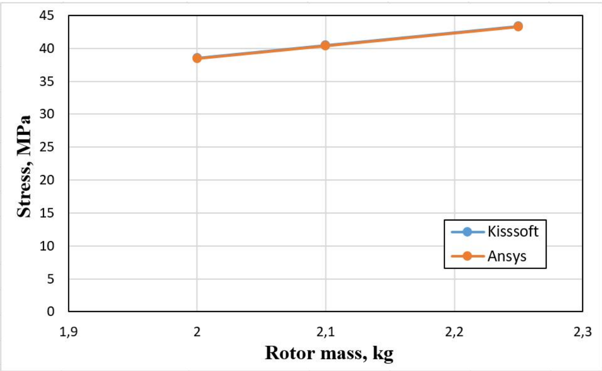

e

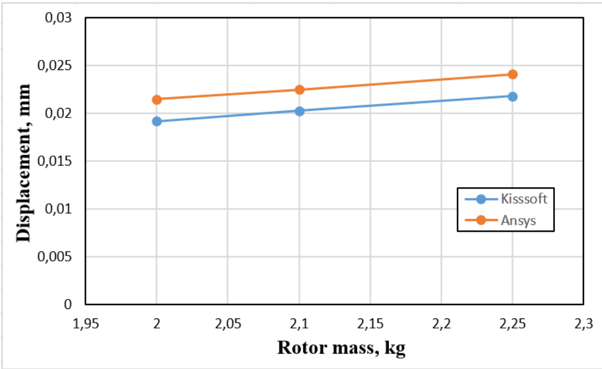

f

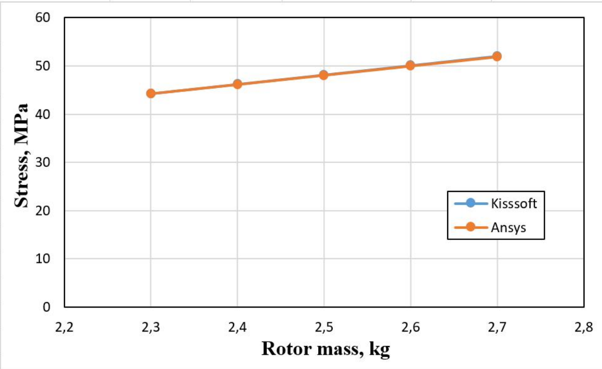

g

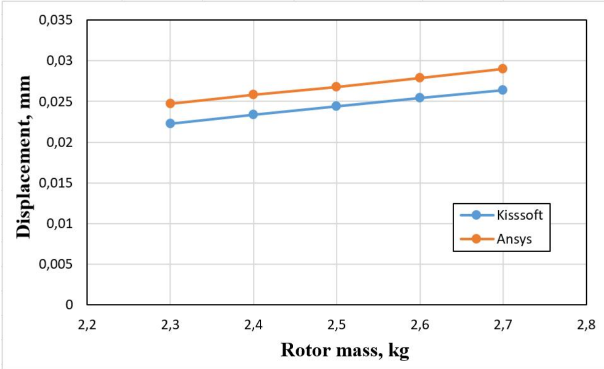

h

Fig. 3. Equivalent stresses *(a, c, e, g)* and total displacements *(b, d, f, h)* calculated for rotors of different masses using KISSsoft and ANSYS

The differences between the calculations of stresses and displacements obtained in KISSsoft and ANSYS are shown in Fig. 4.

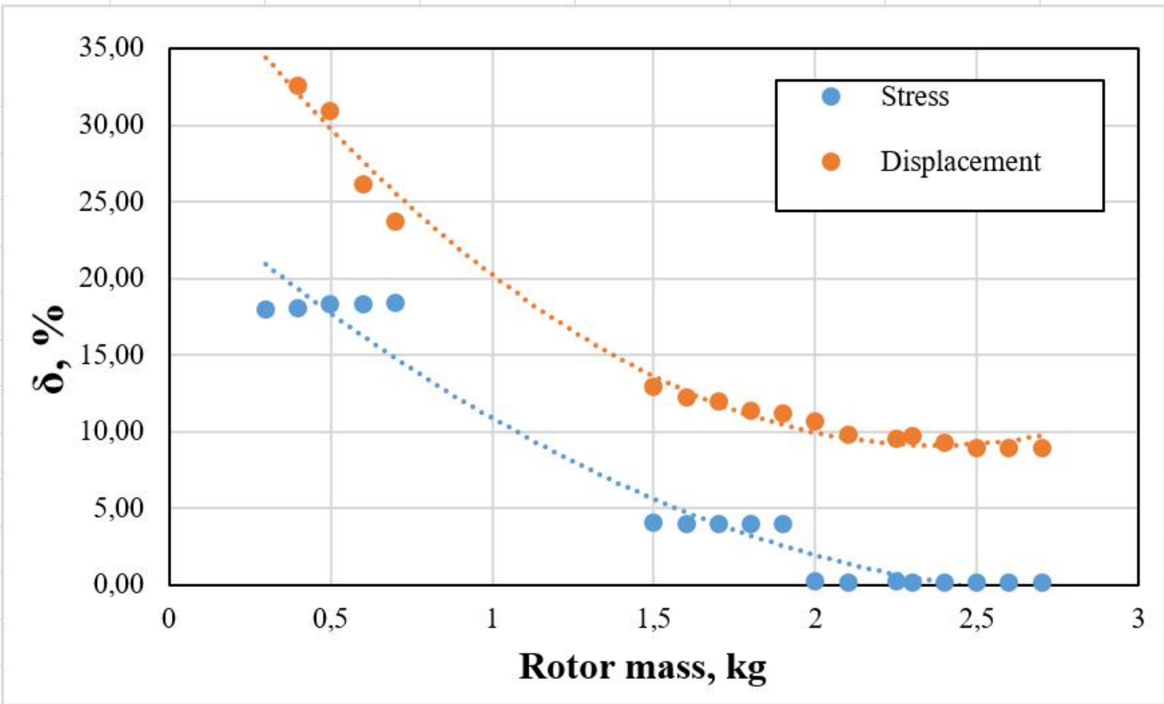

Fig. 4. Modeling accuracy using KISSsoft and ANSYS

2. Numerical modeling of the safety factor using the ANSYS software package

Before you start calculating the safety factor, ANSYS requires the following material characteristics: tensile strength, yield strength, and S-N curve (Stress – Number of cycles). The latter characteristic provides ANSYS with information on how the materials characteristics change during fatigue.

The boundary conditions and shaft loads are the same as for the static strength calculation. Using the model and the corresponding boundary conditions, the safety factor is calculated taking into account the different masses of the rotors.

The modeling results are shown in the form of a scale, with the maximum value being the maximum value of the safety factor and the minimum value being 0. The value of the minimum safety factor for the entire body volume is highlighted separately on the scale. This is the most dangerous point of the calculation model. A positive value of the safety factor is a number higher than 1. The results of numerical modeling using the ANSYS software package are shown in Fig. 5.

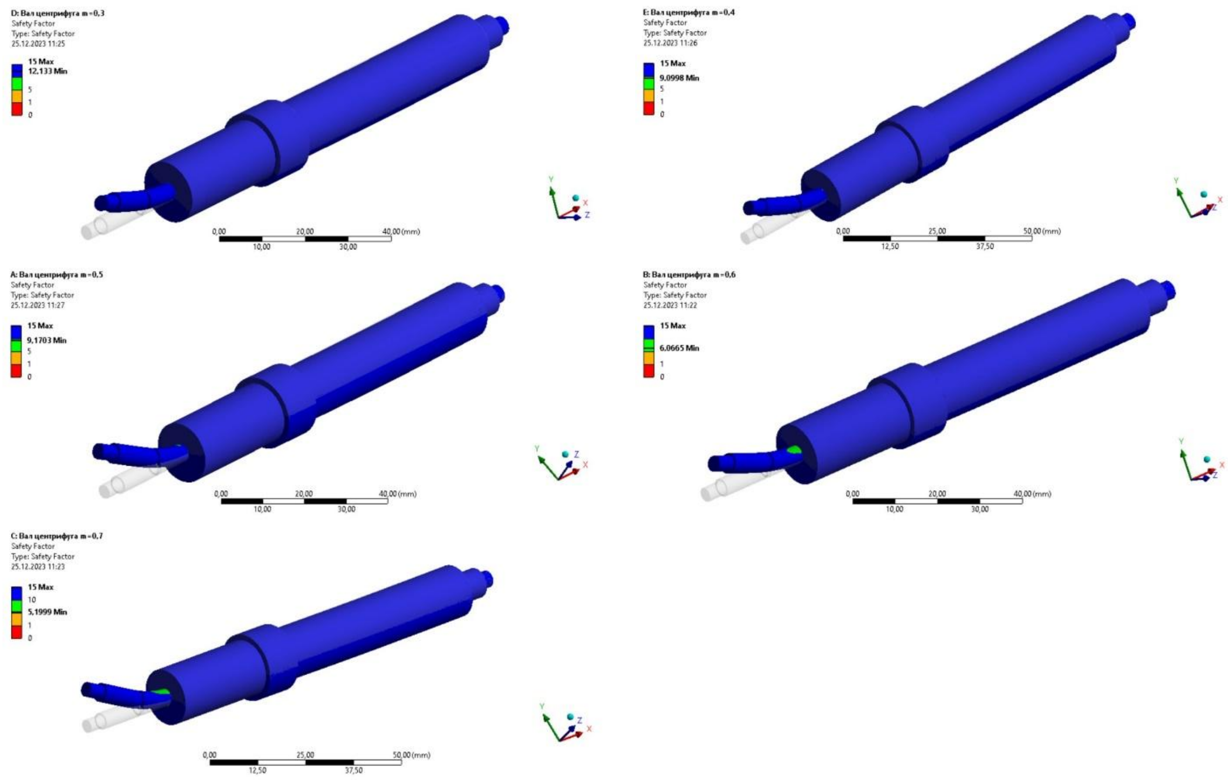

Fig. 5. Safety factor determined using ANSYS

Analytical calculation of the safety factor

To verify the adequacy of the safety factor determination using ANSYS, an analytical calculation was performed for a rotor mass of 0.7 kg. To determine the safety factor, it is necessary to determine the stresses in the dangerous sections of the shaft where the shaft diameter changes. In a dangerous shaft section with a diameter of $d = 4{,}5\ mm$, a bending moment occurs $M_z = 400\ N \cdot mm$ and torque $M_{torque} = 35{,}92\ N \cdot mm$.

Strength characteristics for Steel 45: $\tau_T = 220\ MPa$, $\tau_{-1} = 180\ MPa$, $\sigma_{-1} = 336\ MPa$, $\sigma_B = 700\ MPa$, $\sigma_T = 490\ MPa$.

Shaft processing corresponds to fine grinding ($R_z = 8\ \mu m$). The shaft was not subjected to surface hardening.

The axial moment of resistance is Eq. (1)

$$W_z = \frac{\pi d^3}{32} = \frac{\pi \cdot 4,5^3}{32} = 8,94 \ \ mm^3, \tag{1}$$

while the polar moment of resistance is Eq. (2)

$$W_p = \frac{\pi d^3}{16} = \frac{\pi \cdot 4,5^3}{16} = 17,89 \ \ mm^3. \tag{2}$$

Normal and tangential stresses in the dangerous section are determined according to Eq. (3) and Eq. (4), respectively.

$$\sigma_a = \sigma_{\max} = \frac{M_z}{W_z} = \frac{400}{8,94} = 49,183 \ \ MPa, \tag{3}$$

$$\tau_a = \tau_{\max} = \frac{M_{torque}}{W_p} = \frac{35,92}{17,89} = 2 \ \ MPa. \tag{4}$$

The total safety factor was obtained using the Gough – Pollard formula according to Eq. (5)

$$n = \frac{n_\sigma \cdot n_\tau}{\sqrt{n_\sigma^2 + n_\tau^2}}, \tag{5}$$

where the safety factors determined by normal and tangential stresses are calculated according to Eq. (6) and Eq. (7)

$$n_\sigma = \frac{K_1 \cdot \sigma_{-1}}{K \cdot \sigma_a}, \tag{6}$$

$$n_\tau = \frac{K_1 \cdot \tau_{-1}}{K \cdot \tau_a}. \tag{7}$$

The total coefficients of reduction of the endurance limit for bending and torsion in a dangerous section are determined by formulas Eq. (8) and Eq. (9), respectively:

$$K = \left(\frac{K_\sigma}{K_{d\sigma}} + \frac{1}{K_{F\sigma}} - 1\right) \cdot \frac{1}{K_V \cdot K_A}, \tag{8}$$

$$K = \left(\frac{K_\tau}{K_{d\tau}} + \frac{1}{K_{F\tau}} - 1\right) \cdot \frac{1}{K_V}, \tag{9}$$

where K_σ, K_τ – effective stress concentration factors; $K_{d\sigma}, K_{d\tau}$ – influence factor of the absolute cross-sectional size; $K_{F\sigma}, K_{F\tau}$ – roughness influence factor; K_A – coefficient of influence of technological anisotropy; K_V – coefficient of influence of surface hardening.

Acceptance of $K_\sigma = K_\tau = 1,2$. Due to the absence of surface hardening, the coefficient $K_V = 1$. Coefficient of influence of technological anisotropy $K_A = 0,86$, $K_{d\sigma} = K_{d\tau} = 1$, as the roughness influence factor is calculated according to Eq. (10) and Eq. (11), respectively:

$$K_{F\sigma} = 1 - 0,22 \cdot \left(\lg \frac{\sigma_B}{20} - 1\right) \cdot \lg R_z = 1 - 0,22 \cdot \left(\lg \frac{700}{20} - 1\right) \cdot \lg 8 = 0,89, \tag{10}$$

$$K_{F\tau} = 0,575 \cdot K_{F\sigma} + 0,425 = 0,575 \cdot 0,89 + 0,425 = 0,94. \tag{11}$$

For carbon steels $K_1 = 1$. Taking into account the above coefficients, we calculate the coefficients of endurance limit reduction according to Eq. (8) and Eq. (9):

$$K = \left(\frac{1,2}{1} + \frac{1}{0,89} - 1 \right) \cdot \frac{1}{1 \cdot 1} = 1,32 , \tag{12}$$

$$K = \left(\frac{1,2}{1} + \frac{1}{0,94} - 1 \right) \cdot \frac{1}{1} = 1,27 . \tag{13}$$

The fatigue strength factor for a symmetrical bending cycle is calculated by Eq. (14):

$$n_\sigma = \frac{1 \cdot 336}{1,32 \cdot 49,183} = 5,17 . \tag{14}$$

The factor of safety of static bending strength is calculated according to Eq. (15)

$$n_{T\sigma} = \frac{\sigma_T}{\sigma_{\max}} = \frac{490}{49,183} = 9,96 \cdot \tag{15}$$

Then, $n_\sigma = \min\{n_\sigma, n_{T\sigma}\} = 5,17$.

The fatigue strength factor for symmetrical torsion cycle is calculated by Eq. (16):

$$n_\tau = \frac{1 \cdot 160}{1,27 \cdot 2} = 70,8 . \tag{16}$$

The factor of safety of static torsional strength is calculated according to Eq. (17):

$$n_{T\tau} = \frac{\tau_T}{\tau_{\max}} = \frac{220}{2} = 110 . \tag{17}$$

In summary, $n_\tau = \min\{n_\tau, n_{T\tau}\} = 70,8$.

Using the parameters calculated earlier, we calculate the total safety factor according to Eq. (5) for the dangerous section Eq. (18):

$$n = \frac{5,17 \cdot 70,8}{\sqrt{5,17^2 + 70,8^2}} = 5,16 . \tag{18}$$

The accuracy between the safety factor values calculated analytically and using ANSYS is 0.8 %, indicating the calculation's adequacy.

For the given Steel 45, the safety factor was also calculated according to DIN 743 and Gerber's model Eq. (19):

$$n = \frac{1}{2} \left(\frac{\sigma_B}{\sigma_m} \right)^2 \left(\frac{\sigma_a}{\sigma_{-1}} \right) \left[-1 + \sqrt{1 + \left(2 \frac{\sigma_m \sigma_{-1}}{\sigma_B \sigma_a} \right)^2} \right] . \tag{19}$$

The results of calculations of safety factors taking into account different masses of laboratory centrifuge rotors using Kisssoft, ANSYS software packages and relevant regulatory documents are shown in Fig. 6.

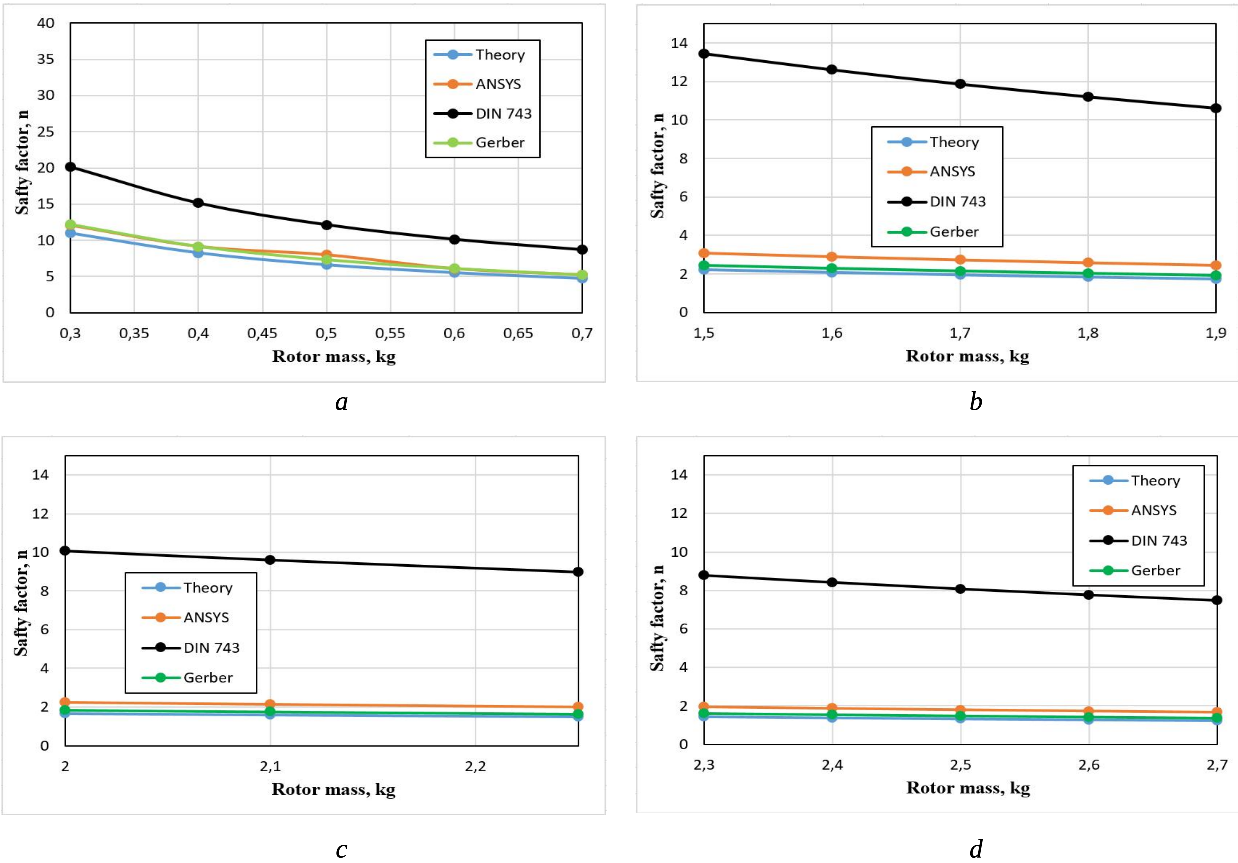

Fig. 6. Comparative analysis of safety factors: *a* – rotor mass 0.3–0.7 kg; *b* – rotor mass 1.5–1.9 kg; *c* – rotor mass 2.0–2.25 kg; *d* – rotor mass 2.3–2.7 kg, respectively

Based on the results of the observations, it is necessary to determine the sample correlation coefficient and check its significance (at the significance level $\alpha = 0,05$), to draw conclusions about the linearity of the studied dependence.

The correlation field of the values of the displacement safety factor for all rotor masses considered in this research paper is shown in Fig. 7.

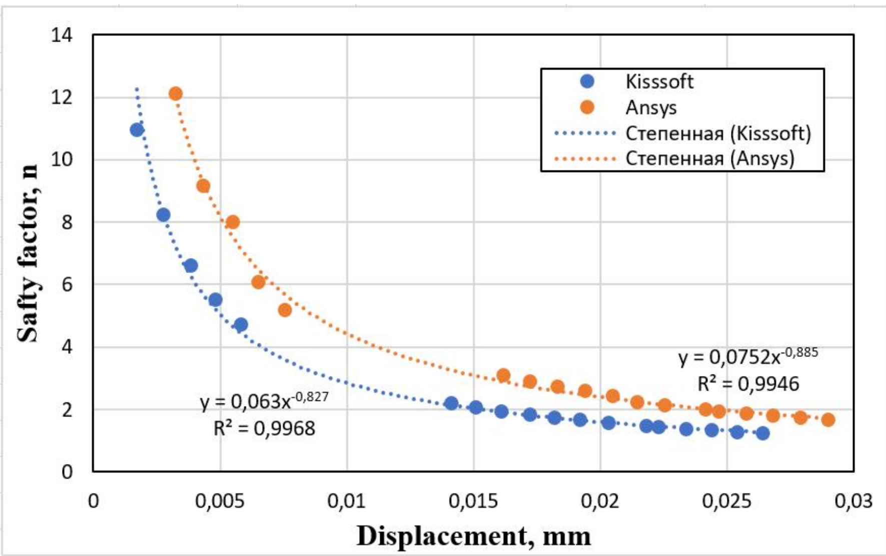

Fig. 7. Correlation field of displacement safety factor values

The sample correlation coefficient is used as a quantitative measure of the linear relationship between two variables. If the value of one variable increases, while the value of the other decreases, then there is a negative correlation, i. e. $r_{xy} < 0$.

To validate the calculations, use the following ratio Eq. (20):

$$\sum (x_i + y_i)^2 = \sum x_i^2 + 2\sum x_i \cdot y_i + \sum y_i^2 . \tag{20}$$

The verification is carried out by substituting the corresponding sums of the values obtained in KISSsoft and ANSYS into Eq. (20). Since both equations' left and right sides coincide, the calculations are correct.

Determine average values obtained in KISSsoft Eq. (21) and Eq. (22)

$$\bar{x} = \frac{\sum x}{n} = \frac{0,28282}{18} = 0,0157 , \tag{21}$$

$$\bar{y} = \frac{\sum y}{n} = \frac{57,211}{18} = 3,1783 . \tag{22}$$

and ANSYS Eq. (23) and Eq. (24), respectively

$$\bar{x} = \frac{\sum x}{n} = \frac{0,32087}{18} = 0,0178 , \tag{23}$$

$$\bar{y} = \frac{\sum y}{n} = \frac{69,7179}{18} = 3,8732 . \tag{24}$$

The value of the sample correlation coefficient is calculated by Eq. (25):

$$r_{xy} = \frac{\sum_{i=1}^{N} x_i \cdot y_i - N \cdot \bar{x} \cdot \bar{y}}{\sqrt{\left(\sum_{i=1}^{N} x_i^2 - N \cdot \bar{x}^2\right) \cdot \left(\sum_{i=1}^{N} y_i^2 - N \cdot \bar{y}^2\right)}} . \tag{25}$$

The value of the sample correlation coefficient for KISSsoft is calculated by Eq. (26):

$$r_{xy} = \frac{0,5356 - 18 \cdot 0,0157 \cdot 3,1783}{\sqrt{\left(0,00563 - 18 \cdot 0,0157^2\right) \cdot \left(319,9218 - 18 \cdot 3,1783^2\right)}} = -0,896 . \tag{26}$$

The value of the sample correlation coefficient for KISSsoft is calculated by Eq. (27):

$$r_{xy} = \frac{0,8369 - 18 \cdot 0,0178 \cdot 3,8732}{\sqrt{\left(0,007 - 18 \cdot 0,0178^2\right) \cdot \left(427,1567 - 18 \cdot 3,8732^2\right)}} = -0,903 . \tag{27}$$

The significance of the sample correlation coefficient is verified by the Student's criterion in the case of a sample with a normal distribution Eq. (28):

$$t_p = \left| r_{xy} \right| \sqrt{\frac{N - 2}{1 - r_{xy}^2}} . \tag{28}$$

The significance of the sample correlation coefficient obtained in KISSsoft is calculated using Eq. (29):

$$t_p = 0,896 \sqrt{\frac{18 - 2}{1 - 0,896^2}} = 1,8903 . \tag{29}$$

The significance of the sample correlation coefficient obtained in ANSYS is calculated using Eq. (30):

$$t_p = 0,903\sqrt{\frac{18-2}{1-0,903^2}} = 1,8981. \tag{30}$$

The resulting values t_p compare to the table value $t_{\alpha,f} = 2,12$ Student's distribution for the significance level $\alpha = 0,05$ for degree of freedom $f = n - 2 = 18 - 2 = 16$.

3. Nonlinear regression from a single factor

Let’s consider a power law of the type $y = a \cdot x^b$, which is widely used in the description of fatigue curves.

It can be reduced to a linear one by logarithmization Eq. (31):

$$\lg y = \lg a + b \cdot \lg x. \tag{31}$$

By making appropriate replacements $Y = \lg y$ and $X = \lg x$, the initial dependency will take the form $Y = b_0 + b_1 \cdot X$, whose coefficients are determined by the minimum squares method. The coefficients of the initial power law are determined as follows $a = 10^{b_0}$, $b = b_1$.

By performing the appropriate transformations $x_i \rightarrow X_i$ and $y_i \rightarrow Y_i$, defined coefficients b_0 Eq. (32) and b_1 Eq. (33) for KISSsoft regression equation

$$b_0 = \frac{\sum y \cdot \sum x^2 - \sum xy \cdot \sum x}{n\sum x^2 - \left(\sum x\right)^2} = -1,4528, \tag{32}$$

$$b_1 = \frac{n\sum yx - \sum y \cdot \sum x}{n\sum x^2 - \left(\sum x\right)^2} = -1,2051. \tag{33}$$

Then the equation describing the values obtained by KISSsoft will be as follows $y = 10^{-1,4528} \cdot x^{-1,2051} = 0,035 \cdot x^{-1,2051}$, in Excel $y = 0,063 \cdot x^{-0,827}$.

Coefficients b_0 Eq. (34) and b_1 Eq. (35) defined for ANSYS regression equation

$$b_0 = \frac{\sum y \cdot \sum x^2 - \sum xy \cdot \sum x}{n\sum x^2 - \left(\sum x\right)^2} = -1,273, \tag{34}$$

$$b_1 = \frac{n\sum yx - \sum y \cdot \sum x}{n\sum x^2 - \left(\sum x\right)^2} = -1,1241. \tag{35}$$

Then the equation describing the values obtained by ANSYS will be as follows $y = 10^{-1,271} \cdot x^{-1,1241} = 0,053 \cdot x^{-1,1241}$, in Excel $y = 0,0752 \cdot x^{-0,885}$.

Conclusions

The following conclusions can be made due to the scientific study of the strength of the PICO21 laboratory centrifuge shaft.

The stresses and displacements obtained in the KISSsoft and ANSYS software systems showed a correlation of results. The difference between the results was found to decrease with increasing rotor mass.

The safety factors for the centrifuge shaft were calculated using KISSsoft, ANSYS, DIN 743, and the Gerber model. It was found that the calculation according to DIN 743:2012 gives overestimated values of the safety factors, which is shown in the corresponding figures. The calculations also revealed that the dependence of the safety factor on displacement is nonlinear.

The Student's criterion tested the significance of the sample correlation coefficient in the case of a sample with a normal distribution. It has been established that for both cases, the calculated values are smaller than the limit values of the table, so it can be assumed that the sample correlation coefficient does not differ significantly from 0, and, accordingly, the relationship between the values is statistically insignificant.

In further research, it is planned to investigate other types of laboratory centrifuges with different rotor shapes and masses.

References

[1] S. M. Ghoneam, et al., "Dynamic analysis of rotor system with active magnetic bearings using finite element method", *International Journal of Engineering Applied Sciences and Technology,* vol. 7, Issue 1, ISSN 2455-2143, pp. 09–16, 2022.

[2] S. D. Dere, and L. Dhamande, "Rotor bearing system FEA analysis for misalignment", *International journal of advance research and innovative ideas in education,* vol. 3, Issue 4, pp. 2102–2112, 2017.

[3] B. Thomas, et al., "Dynamic analysis of functionally graded shaft", *FME Transactions,* vol. 47, Issue 1, pp. 151–157, 2019.

[4] N. Lenin Rakesh, et al., "Stress analysis of a shaft using Ansys", *Middle-east Journal of Scientific Research*, 12 (12), ISSN 1990-9233, pp. 1726–1728, 2012.

[5] B. Gaikwad Rushikesh, and V. Gaur Abhay, "Static and dynamic analysis of shaft (EN24) of foot mounting motor using FEA", *International Journal of Innovations in Engineering Research and Technology,* Vol. 5, Issue 6, ISSN: 2394-3696, pp. 57–70, 2018.

[6] P. Krishna Teja, et al., "Finite element analysis of propeller shaft for automotive and naval application", *International Research Journal of automotive Technology,* vol. 1, Issue 1, ISSN 2581-5865, pp. 8–12, 2018.

[7] A. Asonja, et al., "Analysis of the static behavior of the shaft based on finite method under effect of different variants of load", *Applied Engineering Letters*, vol. 1, No. 1, pp. 8–15, ISSN: 2466-4847, 2016.

[8] S. Noga, et al., "Analytical and numerical analysis of injection pump (Stepped) shaft vibrations using Timoshenko theory", *Acta mechanica et automatica,* vol. 16, No. 3, pp. 215–224, 2022.

[9] P. B. Sob, "Modelling and simulating stress distribution on a centrifugal pump shaft during backpressure", *International Journal of Engineering Research and Technology,* vol. 13, No. 10, ISSN 0974-3154, pp. 2943–2954, 2020.

[10] P. Balon, et al., "Stress concentration analysis of the injection pump shaft", *Advances in Science and Technology Research Journal,* vol. 14, Issue 2, pp. 155–162, 2020.

[11] J. Joshi, et al., "Design analysis of shafts using simulation softwares", *International Journal of Scientific and Engineering Research*, vol. 5, Issue 8, ISSN 2229-5518, pp. 751–761, 2014.

[12] M. J. Jweeg, et al., "Dynamic analysis of a rotating stepped shaft with and without defects", *IOP Conf. Series: Materials Science and Engineering, 3rd International Conference on Engineering Sciences,* Kerbala, Iraq, 2020, vol. 671.

[13] S. Culafic, and D. Bajic, "Analytical and numerical analysis of shafts' stress and strain states of the hydro-power unit", *International Scientific Journal "Machines. Technologies. Materials",* vol. XV, Issue 8, pp. 294–298, 2021.

[14] C. Gong, et al., "High-strength rotor design for ultra-high speed switched reluctance machines", in *IEEE Transactions on Industry Applications*, 2020, vol. 56, Issue: 2, pp. 1432–1442.

[15] M. E. Gerlach, et al., "Mechanical stress and deformation in the rotors of a high-speed PMSM and IM", *Elektrotechnik und Informationstechnik*, vol. 138, Issue 2, pp. 96–109, 2021.

[16] N. F. Timerbaev, et al., "Software systems applications for shaft strength analysis in mechanical engineering", *Procedia Engineering*, vol. 206, pp. 1376–1381, 2017.

[17] N. Rasovic, et al., "Design and analysis of steel reel shaft by using FEA", *Tehnicki vjesnik*, vol. 26, Issue 2, pp. 527–532, 2019.